Electronic Supplementary Material (ESI) for Catalysis Science & Technology.
This journal is © The Royal Society of Chemistry 2024

Supplementary Material

Enhanced Photocatalytic Performance of Thiophene-Modified Graphitic Carbon Nitrides as Donor-Acceptor Conjugated Organic Polymers

Yanan Liu[a], Shuaishuai Lu[a], Tong Yuan[a], Siyuan Wang[a], Janina Bahnemann[b, c], Fang Jiang[a, *], Huan Chen[a, *]

[a] *Key Laboratory of Jiangsu Province for Chemical Pollution Control and Resources Reuse, School of Environmental and Biological Engineering, Nanjing University of Science and Technology, Nanjing 210094, China.*

[b] *Institute of Physics, University of Augsburg, 86159 Augsburg, Germany.*

[c] *Centre for Advanced Analytics and Predictive Sciences (CAAPS), University of Augsburg, 86159 Augsburg, Germany.*

*Corresponding author:

E-mail: fjiang@njust.edu.cn, hchen404@njust.edu.cn

2. Experimental Section

2.1 Materials

2,5-thiophenedicarboxylic acid (TA), 1-Hydroxy-7-azabenzotriazole (HOAT), Urea, 1-Ethyl-3-(3-dimethylaminopropyl) carbodiimide hydrochloride (EDC·HCl), *N*,*N*-Dimethylformamide (DMF), Triethylamine are purchased from Chinese medicine. All chemical reagents were used as received without any purification.

2.2 Preparation of photocatalysts

2.2.1 Synthesis of S-g-C_3N_4

6g urea and 20 mg TA were directly added to 50 mL methanol, and then stirred at 80 °C to remove water. The resulting solids are transferred to a crucible completely wrapped in aluminum foil and then calcined at 550 °C for 4 hours at a ramp rate of 5.0 °C min^{-1}. After cooling to room temperature, the orange powder solids will be obtained. The samples were centrifuged and washed, dried at 60 °C overnight, and harvested as S-g-C_3N_4. The original graphite carbon nitride was prepared by directly heating 6 g urea at 550 °C for 4 h at the same heating rate, and marked as S-g-C_3N_4.

2.2.2 Synthesis of S-g-C_3N_4/TA

Pour anhydrous dimethylformamide (DMF, 50 mL) into a 100 ml flask. The thiophene derivative carboxylic acid (1 mmol) was dispersed in DMF under vigorous stirring. The mixture was cooled in an ice bath at 0°C and 1-hydroxy-7-azabenzotriazole (HOAt, 0.389g, 2.86 mmol) was added. N- (3-dimethylaminopropyl) -N-ethylcarbodiimide hydrochloride (EDC, 0.548g, 2.86 mmol) was poured into the solution and activated for 30 min. Then, S-g-C_3N_4 (0.1g) was added and the pH was adjusted to 8 with triethylamine (TEA, 15 ml). After 10 minutes, remove the ice bath and react quickly for 15 hours [1]. Washed three times with saturated sodium bicarbonate, sodium chloride and deionized water, dried in vacuum at 50 °C, recorded as 1mmol S-g-C_3N_4/TA. Under the same conditions, 0.7mmol, 1.3mmol, 2.6mmol and 3.9mmol samples were prepared in turn.

2.3 Typical procedure for photocatalytic test

A multi-channel photoreactor equipped with a 500 W Xe lamp was used to simulate sunlight for photocatalytic degradation of BPA. Usually, the photocatalyst was administered in the amount of 0.02 g and the BPA solution was 50 mL. In order to avoid the effect of photocatalyst on the adsorption of BPA, the adsorption equilibrium experiment was performed without light before the start of the reaction. Then, the reaction system after the adsorption equilibrium was sampled at equal intervals during the light time. After sampling was completed, samples were analyzed at 230 nm on a high-performance liquid chromatograph (E2685, Waters) equipped with a Waters XBridge-C18 column (250 mm×4.6 mm, 5 μm) and a UV-Vis detector (2489, Waters).

For the cycling test, the catalyst was centrifuged, washed with absolute alcohol and then dried at 50 °C in vacuum oven for 12 h.

2.4 Quenching experiments

Different scavengers such as sodium oxalate, 2,2,6,6-tetramethylpiperidine-1-oxyl (TEMPO), furfuryl alcohol and isopropanol were used as scavengers for holes (h^+), superoxide radicals ($\cdot O_2^-$), singlet oxygen ($^1O_2$) and hydroxyl radicals (·OH), respectively. In the free radical trapping experiments, 10 mM of different trapping agents and catalysts were successively added into the photocatalytic reaction system. After the dark reaction adsorption equilibrium was completed, 1 mL of the sample was taken every 30 min and passed through a 0.22 μm filter membrane. Afterwards the samples were tested in the liquid phase using the same method.

2.5. Characterizations

X-ray diffraction (XRD) tests were analyzed on a Bruker D8-Advance X-ray diffractometer with Cu Kα radiation source from 5 to 80 degree with the scanning rate of 6°/min. A Nicolet iS10 was employed to obtain the Fourier transform infrared spectroscopy (FT-IR). X-ray photoelectron spectroscopy (XPS) was operated on a Thermo ESCALAB 250XI. Transmission electron microscope (TEM) was furnished

by the JEOL JEM 2100 F electron microscope. N_2 adsorption-desorption tests were carried out on the Autosorb iQ Station 2 at 77 K. Ultraviolet-visible absorption spectra (UV–vis DRS) were determined by Shimadzu UV-3600 with test range from 200 to 800 nm using $BaSO_4$ as a reference.

2.6. Photoelectrochemical measurements

All the photoelectrochemical measurements were performed on an electrochemical workstation (CHI 660E, CH Instruments Inc., Shanghai). The working electrodes were prepared as follows. 2 mg of catalyst was dispersed in 1.0 mL absolute ethanol and 20 μL Nafion mixture solution, which was ultrasonically dispersed for 60 min, and then 100 μL of mixture solution was dropped onto the ITO with 1 × 1 cm^2 illuminated area and dried at room temperature. In all the electrochemical experiments, a three-electrode cell with as-prepared working electrodes, Pt plate as a counter electrode, Ag/AgCl as a reference electrode as well as 0.2 M Na_2SO_4 solution as electrolyte solution was used, respectively. The transient photocurrent-time (I-t) was measured using the 500 W Xe lamp with lamp on and off at a time interval of 20s. The electrochemical impedance spectroscopy (EIS) measurements were performed over a frequency range from 1 Hz to 10^5 Hz with 5 mV amplitude. The Mott-Schottky (M–S) plots were measured at frequencies of 1000, 1500, 2000 Hz.

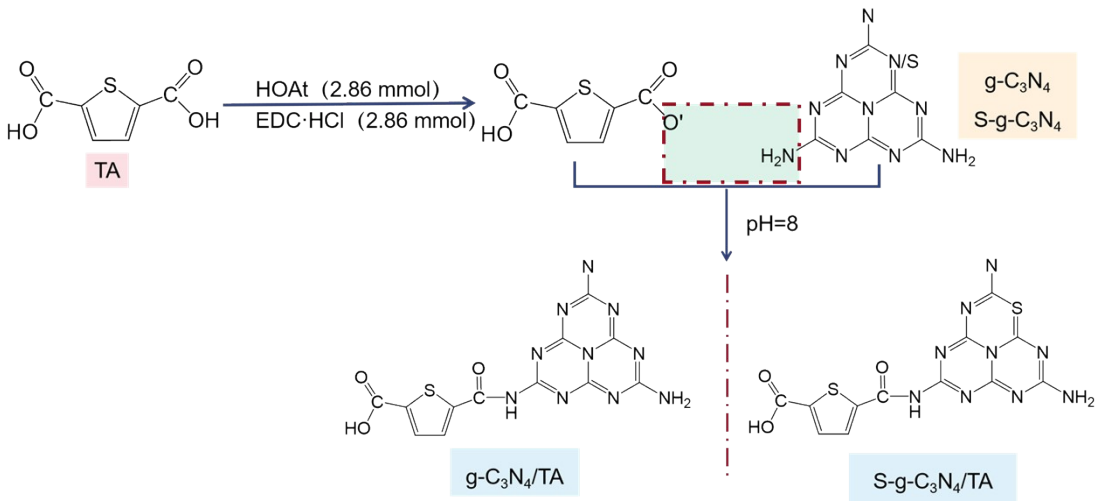

Schematic S1. Synthesis schematic of g-C_3N_4/TA and S-g-C_3N_4/TA

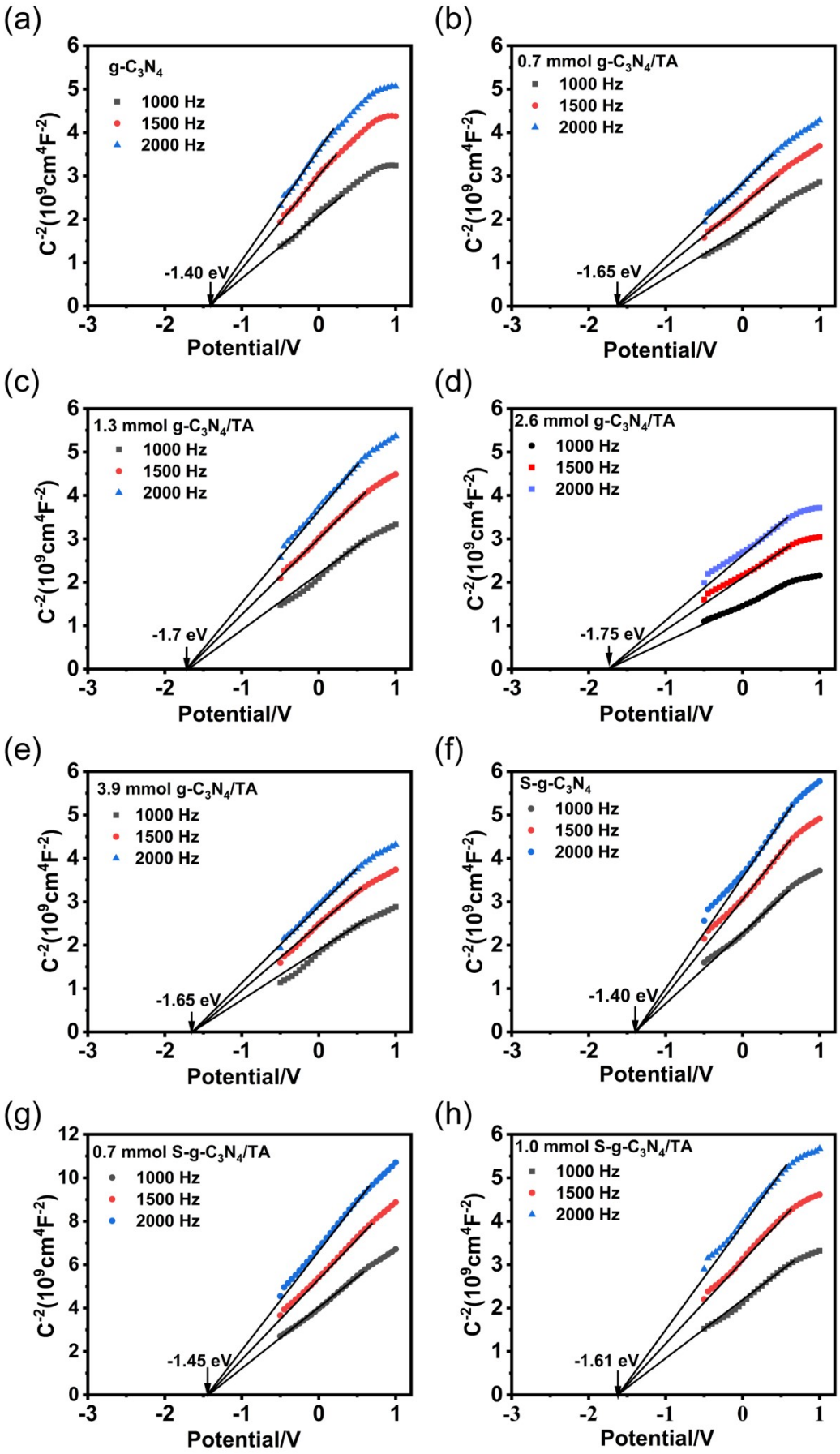
(a)
g-C3N4
1000 Hz
1500 Hz
2000 Hz
-1.40 eV
C-2(109cm4F-2)
Potential/V
(b)
0.7 mmol g-C3N4/TA
1000 Hz
1500 Hz
2000 Hz
-1.65 eV
C-2(109cm4F-2)
Potential/V
(c)
1.3 mmol g-C3N4/TA
1000 Hz
1500 Hz
2000 Hz
-1.7 eV
C-2(109cm4F-2)
Potential/V
(d)
2.6 mmol g-C3N4/TA
1000 Hz
1500 Hz
2000 Hz
-1.75 eV
C-2(109cm4F-2)
Potential/V
(e)
3.9 mmol g-C3N4/TA
1000 Hz
1500 Hz
2000 Hz
-1.65 eV
C-2(109cm4F-2)
Potential/V
(f)
S-g-C3N4
1000 Hz
1500 Hz
2000 Hz
-1.40 eV
C-2(109cm4F-2)
Potential/V
(g)
0.7 mmol S-g-C3N4/TA
1000 Hz
1500 Hz
2000 Hz
-1.45 eV
C-2(109cm4F-2)
Potential/V
(h)
1.0 mmol S-g-C3N4/TA
1000 Hz
1500 Hz
2000 Hz
-1.61 eV
C-2(109cm4F-2)
Potential/V

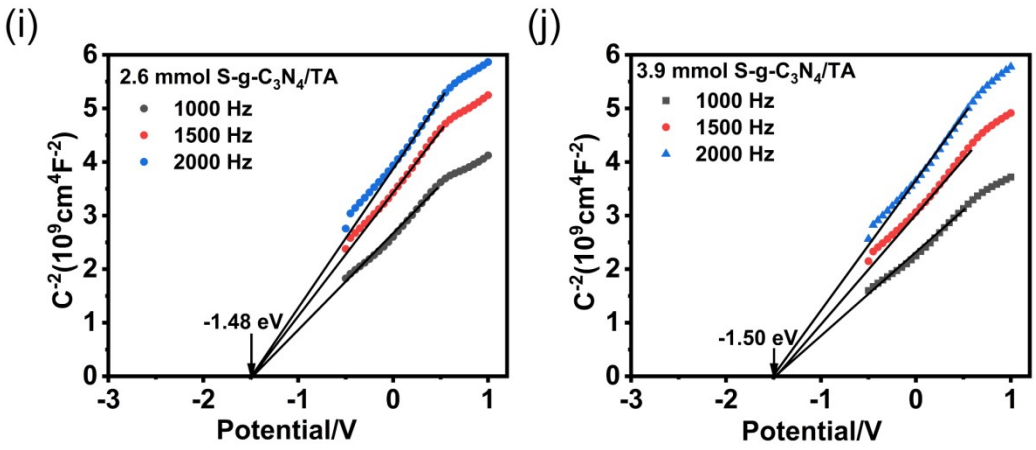

Fig. S1. Mott-Schottky plots of g-C_3N_4 (a), 0.7 mmol g-C_3N_4/TA (b), 1.3 mmol g-C_3N_4/TA (c), 2.6 mmol g-C_3N_4/TA (d), 3.9 mmol g-C_3N_4/TA (e), S-g-C_3N_4 (f), 0.7 mmol S-g-C_3N_4/TA (g), 1.0 mmol S-g-C_3N_4/TA (h), 2.6 mmol S-g-C_3N_4/TA (i) and 3.9 mmol S-g-C_3N_4/TA (j).

The relative positions of catalyst HOMO and LUMO levels were determined by cyclic voltammetry, and the g-C_3N_4/TA samples resulted in -5.7 ± 0.1 eV for HOMO and -2.6 ± 0.1 eV for LUMO (Fig. 7c, d). S-g-C_3N_4/TA samples resulted in -5.6 ± 0.1 eV for HOMO and -3.0 ± 0.1 eV for LUMO. Calculations are made according to the following formula: [2]

$$E_{LUMO}(eV) = -\left[4.8 - E_{1/2}(Fc, Fc^{+}) + E_{red,onset}\right] \quad \text{Equation (1)}$$

$$E_{HOMO}(eV) = -\left[4.8 - E_{1/2}(Fc, Fc^{+}) + E_{\mathrm{ox},onset}\right] \quad \text{Equation (2)}$$

Electrochemical measurements were conducted on a three- electrode cell system using as electrolyte 0.1 M tetra-n-butylammonium hexafluorophosphate in acetonitrile. The CV curves were calibrated using the ferrocene/ferrocenium (Fc/Fc_+) redox couple as an external standard which was measured under same condition before and after the measurement of samples. The calibration value is 0.4 eV.

The data in the table were obtained according to the following formula.

$$Evac = -4.5 - E_{NHE} \quad \text{Equation (3)}$$

Table S1 CV estimation of bandgap, CB, and VB potentials

	g-C_3N_4	0.7 mmol g-C_3N_4/TA	1.3 mmol g-C_3N_4/TA	2.6 mmol g-C_3N_4/TA	3.9 mmol g-C_3N_4/TA
Band gap	2.9	2.85	2.95	2.95	2.9
CB	-1.8	-1.75	-1.8	-1.75	-1.7

VB	1.1	1.1	1.15	1.2	1.2
	S-g-C_3N_4	0.7 mmol S-g-C_3N_4/TA	1.0 mmol S-g-C_3N_4/TA	2.6 mmol S-g-C_3N_4/TA	3.9 mmol S-g-C_3N_4/TA
Band gap	2.6	2.63	2.62	2.6	2.6
CB	-1.5	-1.52	-1.55	-1.53	-1.55
VB	1.1	1.11	1.07	1.07	1.05

Table S2 Percentage of C1s peak area in XPS

	C-C/C=C（%）	**N-C=N（%）**	**C-S（%）**
g-C_3N_4	17%	83%	
g-C_3N_4/TA	17%	79%	4%
S-g-C_3N_4	37%	59%	4%
S-g-C_3N_4/TA	23%	69%	8%

Table S3 Percentage of N1s peak area in XPS

	C-$NH_X(N_1)$（%）	**C-N=C(N_2)（%）**	**N-$C_3(N_3)$（%）**	**π excitation**
g-C_3N_4	8.8%	72.2%	12.7%	6.3%
g-C_3N_4/TA	8.3%	74.8%	12.8%	4.0%
S-g-C_3N_4	8.0%	72.1%	13.1%	6.8%
S-g-C_3N_4/TA	6.7%	70.7%	15.4%	7.1%

Table S4 Percentage of S peak area in XPS

	C-S-C（%）	**C-SO_X-C（%）**
S-g-C_3N_4	43.2%	56.8%
S-g-C_3N_4/TA	57.3%	42.7%

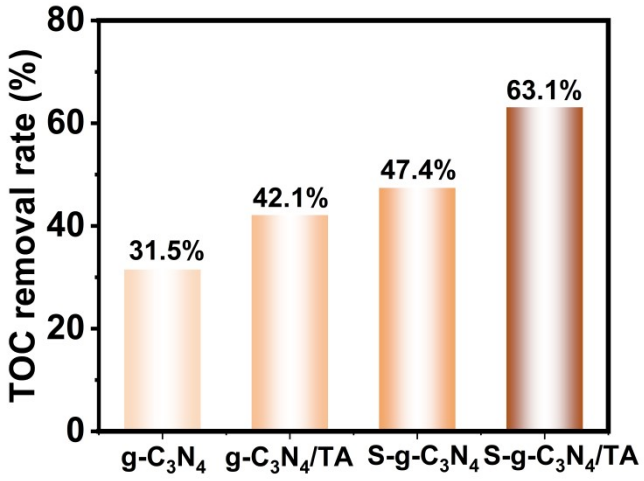

Fig. S2 The TOC removal effect diagram of BPA degradation by g-C_3N_4, g-C_3N_4/TA, S-g-C_3N_4 and S-g-C_3N_4/TA in 180 min.

Table S5 Comparison of the performance of photocatalysts on the degradation of BPA

Materials	Catalyst dosage (g/L)	BPA concentration (mg/L)	BPA volume (mL)	reaction time (h)	TOC degradation rate (%)	References
$MoS_2/SnIn_4S_8$	0.5	10	40	8	~20%	[3]
Gd^{3+} over Bi_2O_3	1	25	100	6	70%	[4]
GCN/rGO	1	5	40	4	80%	[5]
$CoFe_2O_4$-g-C_3N_4	0.4	12.5	50	2	55%	[6]
P(HEA-co-HAM)-CdS	2	50	10	5	58%	[7]
S-g-C_3N_4/TA	0.4	20	50	3	63.1%	This work

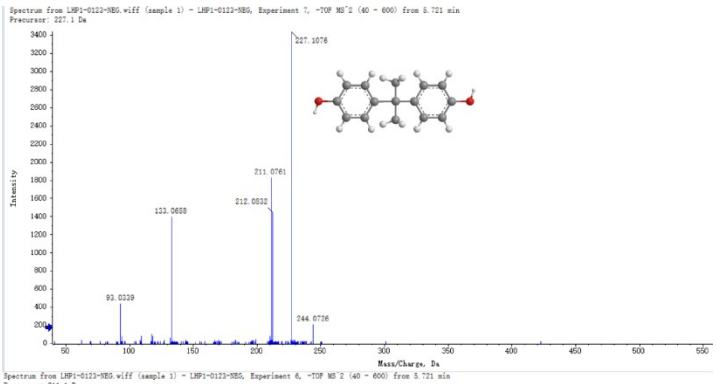
Spectrum from LMP1-0123-NEG.wiff (sample 1) - LMP1-0123-NEG, Experiment 7, -TOF MS^2 (40 - 600) from 5.721 min
Precursor: 227.1 Da
227.1076
211.0761
212.0832
133.0658
93.0339
244.0726
Intensity
Mass/Charge, Da

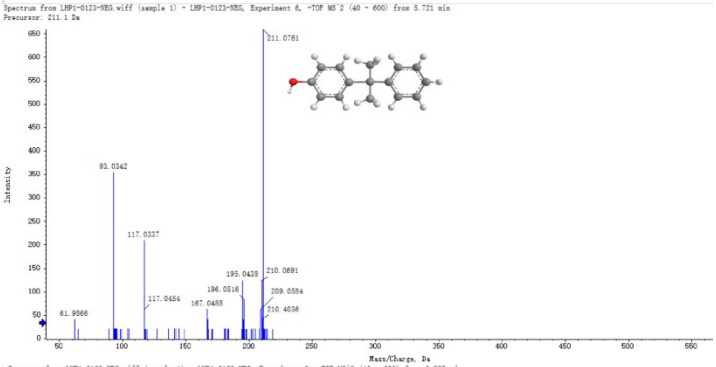
Spectrum from LMP1-0123-NEG.wiff (sample 1) - LMP1-0123-NEG, Experiment 6, -TOF MS^2 (40 - 600) from 5.721 min
Precursor: 211.1 Da
211.0761
93.0342
117.0337
195.0428
210.0691
196.0516
209.0584
117.0454
167.0458
210.4036
61.9866
Intensity
Mass/Charge, Da

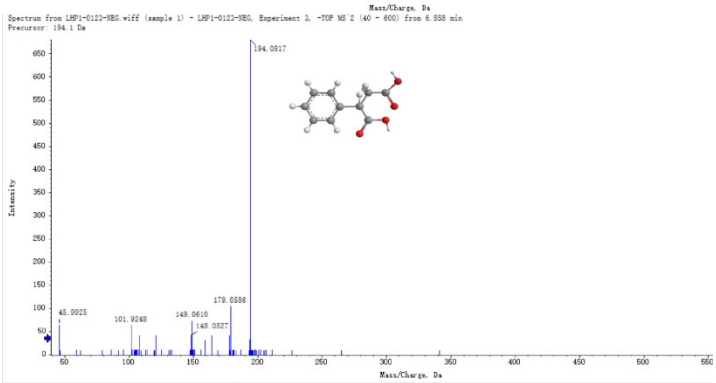
Spectrum from LMP1-0123-NEG.wiff (sample 1) - LMP1-0123-NEG, Experiment 3, -TOF MS^2 (40 - 600) from 6.838 min
Precursor: 194.1 Da
194.0817
179.0586
45.0025
101.9248
149.0610
148.0527
Intensity
Mass/Charge, Da

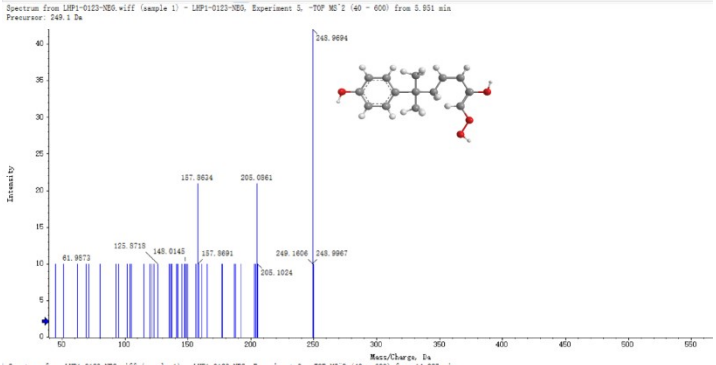
Spectrum from LMP1-0123-NEG.wiff (sample 1) - LMP1-0123-NEG, Experiment 5, -TOF MS^2 (40 - 600) from 3.951 min
Precursor: 249.1 Da
248.9894
157.9634
205.0861
123.8718
148.0145
157.8691
61.9873
249.1606
248.9967
205.1024
Intensity
Mass/Charge, Da

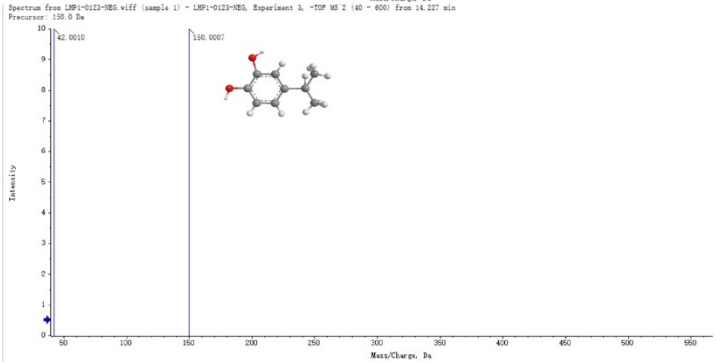
Spectrum from LMP1-0123-NEG.wiff (sample 1) - LMP1-0123-NEG, Experiment 3, -TOF MS^2 (40 - 600) from 14.227 min
Precursor: 150.0 Da
42.0010
150.0007
Intensity
Mass/Charge, Da

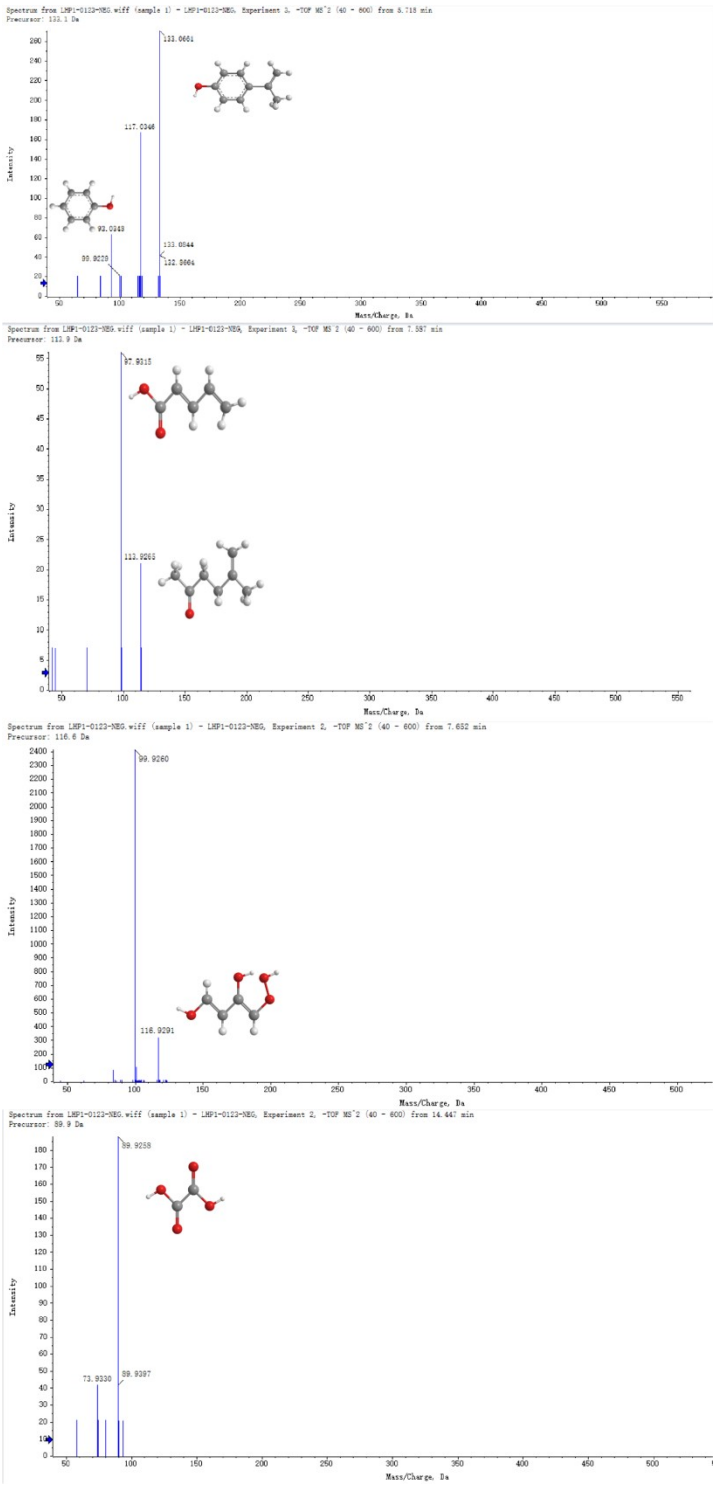

Fig. S3. Possible degraded/oxidized products of BPA determined by HPLC-MS.

Table. S6 Reaction intermediates identified by HPLC-MS.

Number	Chemical name	m/z	Molecular structure
1	BPA	228	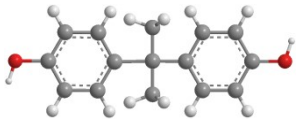
2	4-Isopropylphenol	212	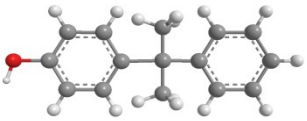
3	2-Phenylsuccinic acid	195	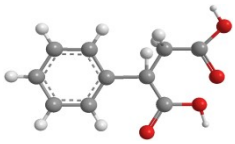
4	4-((4Z,6Z)-7-hydroperoxy-6-hydroxy-2-methylhepta-4,6-dien-2-yl)phenol	250	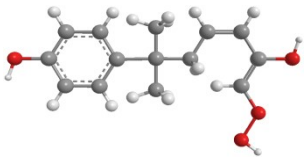
5	4-(2-hydroxypropan-2-yl)phenol	151	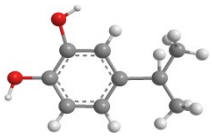
6	4-Isopropenylphenol	134	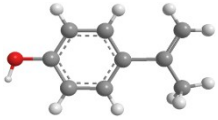
7	Phenol	94	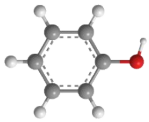
8	2,5-Hexanedione	114	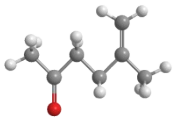
9	Prop-1-en-2-ylbenzene	117	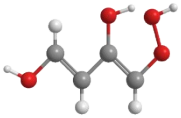
10	oxalic acid	90	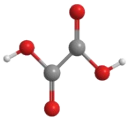

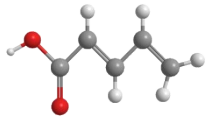

References

1. A. Privitera, M. Righetto, D. Mosconi, F. Lorandi, A. A. Isse, A. Moretto, R. Bozio, C. Ferrante and L. Franco, *Phys Chem Chem Phys*, 2016, **18**, 31286-31295.
2. N. M. Padial, J. Castells-Gil, N. Almora-Barrios, M. Romero-Angel, I. da Silva, M. Barawi, A. García-Sánchez, V. A. de la Peña O'Shea and C. Martí-Gastaldo, *J. Am. Chem. Soc.*, 2019, **141**, 13124-13133.
3. R. Weng, F. Tian, Z. Yu, J. Ma, Y. Lv and B. Xi, *Chemosphere*, 2021, **285**, 131542.
4. G. H. Munshi, M. Aslam, M. G. Alam, S. Chandrasekaran, M. T. Soomro, I. M. I. Ismail and A. Hameed, *Materials Today Communications*, 2023, **35**, 106005.
5. Y.-H. Chen, B.-K. Wang and W.-C. Hou, *Chemosphere*, 2021, **278**, 130334.
6. Ö. Görmez, E. Yakar, B. Gözmen, B. Kayan and A. Khataee, *Chemosphere*, 2022, **288**, 132663.
7. M. Rani, Rachna and U. Shanker, *Environmental Technology & Innovation*, 2020, **19**, 100792.